Ceramic Structures by Selective Laser Sintering of Microencapsulated, Finely Divided Ceramic Materials

N. K. Vail and J. W. Barlow
Department of Chemical Engineering
The University of Texas at Austin

Abstract

The feasibility of producing ceramic green parts by Selective Laser Sintering from microencapsulated, finely divide ceramic powders has been reported in an earlier paper. Post-processing of a silica/zirconium orthosilicate system and an alumina system, both utilizing a polymer binder in the form of a coating, are discussed in this paper. Ceramic green parts require post-processing to remove the intermediate polymer binder and to impart strength properties to the ceramic bodies. In this paper, the use of ceramic cements and high temperature firing to realize strengths will be discussed. The effects of cement concentration and controlled drying rates on the strengths and dimensional accuracy of the ceramic bodies are also discussed.

Introduction

In recent years, in order for manufacturers to remain competitive, the need for the capability to rapidly prototype and develop objects has greatly increased. Concurrently, several novel approaches have emerged to realize rapid prototyping and development [1]. Most are processes which work by the layerwise addition of material. Polymers, with various properties, are the most predominant materials used by these processes although some are attempting to use high temperature materials such as ceramics and metals. While processes using the later materials are a few years away from fully realizing their goals, those processes which use polymers are making rapid progress in areas of application and resulting part quality.

Selective Laser Sintering (SLS) is one of these processes which has gained prominence in the area of rapid prototyping within the past few years. This process has proven itself extremely suitable to the handling of polymer materials. However, its usefulness is not limited to these materials. SLS has been successfully applied to other materials systems which either use an intermediate low-temperature binder or use direct sintering of high-temperature materials [2,3].

The use of low-temperature binders, namely, polymer binders in ceramic systems, has been described and proven effective as a means of producing shapes with good green strength, improved surface finish, and fine feature definition [4]. These "green" parts, however, require post-processing to remove the polymer binder and to impart greater strength. Greater strengths can be achieved by high-temperature firing to sinter the ceramic material. This method involves a certain amount of densification which results in shrinkage of the piece. Since most of the ceramic green pieces produced by SLS currently exhibit low relative densities, on the order of 40-50%, shrinkages involved to achieve desired strengths are large.

An alternative to high-temperature sintering is the use of ceramic cements to achieve strength. Infiltrating a green structure with a ceramic cement then processing it to remove

the polymer binder and cure the cement, is the proposed method of producing ceramic parts with good strengths and little dimensional change.

Materials and Methods

A sample of UCAR 430 Acrylic Polymer Latex was obtained from Union Carbide Corporation. UCAR 430 Latex is a styrene-methylmethacryate copolymer paint base. A sample of a polymethylmethacrylate (PMMA) latex exhibiting specific melt flow characteristics was provided by Rhome-Haas. The properties of these polymers are listed in Table 1. Silica and zircon were obtained from Ransom and Randolf, Inc. as Rancosil #4 and Zircon Flour 325, respectively. A sample of alumina was provided by Lanxide Corporation. The ceramic characteristics are listed in Table 2.

Three grades of inorganic ceramic cements were obtained from Aremco Products, Inc. These were Cerama-Bind™ products grades 542, 643, and 644. These binders are primarily silicate colloids which, upon curing, provide temperature resistances to 1750°C. In addition to these binders, three samples of *Ludox*® Colloidal Silica were provided by E.I. duPont de Nemours & Co., Inc. These colloids and their properties are listed in Table 3.

Table 1. Polymer properties.

Polymer Latex	Particle Size, (nm)	Solids, (wt. %)	T_g, (°C)	M_w	Melt Index, (g/10min)
UCAR 430	320	45	45	200000	N.A.
PMMA	290	50	93	2000	20.0

Table 2. Ceramic powder characteristics.

Material	Purity, (%)	Particle Size, (μm)	Density, (g/cc)
Rancosil #4	99.8	63.0	2.25
Zircon Flour	99.8	17.0	4.56
Alumina	99.0	15.0	3.98

Table 3. *Ludox*® Colloidal Silica properties

Grade	Type	Particle Size, (nm)	Solids, (wt. %)
SM	Silica	7	30
TM	Silica	22	50
AM	Silica/Alumina	12	30

Three samples of polymer coated ceramic materials were prepared using the method reported previously [4]. These samples included silica/zircon coated with UCAR 430, silica/zircon coated with PMMA, and alumina coated with PMMA. The material make-up and coating conditions for these samples are listed in Table 4. Samples #34 and #35 were admixed with pure ceramic materials to reduce their respective polymer contents to 15% vol (7.5 wt. % and 5.0 wt. %, respectively). This was done to further reduce the polymer content of the material, to enhance powder packing, and to introduce uncoated particle surfaces for interaction with ceramic cements during penetration. Admixing of polymer coated and uncoated particles was shown to improve observed bed densities without

125

significantly affecting the strength of the resultant SLS green part as long as the pure particle content was kept low [4].

Table 4. Coated ceramic powder make-up and coating conditions.

Sample #	Material	Content, wt. (vol.)	Feed Solids (wt. %)	Temp. (°C) Inlet	Temp. (°C) Outlet	Atomizer Speed, rpm
28	Silica	60.0 (62.8)	50	150	60	37500
	Zircon	30.0 (14.7)				
	UCAR 430	10.0 (22.5)				
34	Silica	60.0 (65.0)	50	175	82	37500
	Zircon	30.0 (15.2)				
	PMMA	10.0 (19.8)				
35	Alumina	90.0 (80.0)	50	175	88	37500
	PMMA	10.0 (20.0)				

Selective Laser Sintering

All materials were SLS processed using an SLS™ Model 125 equipped with a 25 watt CO_2 laser. SLS processing occurred in a nitrogen environment and with elevated bed temperatures. SLS processing conditions for the three powder samples are listed in Table 5. Several parts were made from each powder sample. Specifically, test bars with dimensions 1"x5" and 1"x3" with total thicknesses ranging from 20-80 layers were produced as were square parts with dimensions ranging from ¾" to 2" with thicknesses of ¼".

Table 5. Selective Laser Sintering operating conditions

Sample	Power, (W)	Layer Thickness, (mil)	Beam Spacing, (mil)	Scan Speed, (ips)	Temp., (°C) Bed	Temp., (°C) Air
28	12	5, 6	2, 5, 8	150	40, 50, 60	90
34	10	5	2	100	70	70
35	10	3, 4	2	20-100	80	35

Post-Processing of SLS Parts

SLS processed parts were brushed to remove loose powder and their densities were determined. Test samples were subsequently infiltrated with a ceramic cement material. Infiltration was performed simultaneously by capillary action and by dripping the infiltrating material onto part edges. Once a part had been infiltrated it was allowed to dry for an extended period at ambient conditions. When drying was complete residual moisture was removed by firing for one hour at 200°C. Polymer binder was then removed by firing for an additional one hour at 400°C. Following removal of polymer binder, parts were re-infiltrated with cement material, dried, and residual moisture removed by firing for an additional one hour at 200°C. The mass of each part was measured at the end of each step during the post-processing. Following the second curing, the strengths of several parts were determined by four-point bend analysis. Other samples were fired at high temperature using the firing cycle shown in Figure 1. Strengths of these fired parts were also determined by a four-point bend analysis.
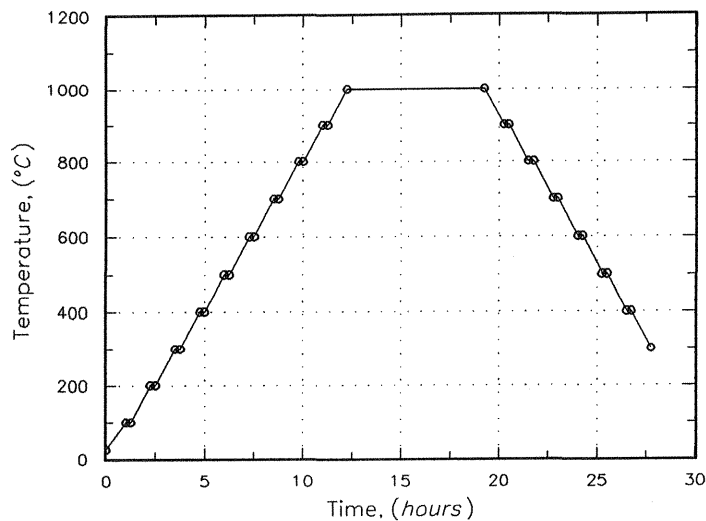
126

Figure 1. High temperature firing cycle.

Results and Discussion

All test parts made from the three powder samples had sufficient green strengths to permit handling and exhibited good surface finishes as well as good edge definition. Not surprisingly, test parts made from the alumina powder sample exhibited finer features due to its smaller particle size. Test bars made from each of the three powder samples, #28, #34, and #35, were determined to have relative densities of 39.5±1.4, 41.3±1.4, and 45.1±1.2, respectively. Densities increased slightly with increased part thicknesses.

Penetration experiments were conducted on parts made from all three powder samples. Initially, test pieces made from powder sample #28 (UCAR coated silica/zircon) were penetrated with the Cerama-Bind™ materials. However, during the first penetration tests of these pieces, it became apparent that the viscosities and surface tensions of these cements were too great to permit effective penetration. In a 1"x3" bar, infiltrated by capillary action, the penetration front would scarcely advance ¼" before no further movement of the front could be observed.

The viscosities and surface tensions were altered by diluting the cement materials with water. None of the three grades, however, was stable to the addition of water although the 643 grade took at least 24 hours to gel. Even when diluted to 50% by volume with water the 643 still did not penetrate test samples effectively. Subsequently, the binders were diluted with methanol to further reduce their surface tension. Only the 644 grade proved stable to the addition of methanol and penetration tests using this solution proved excellent. Test bars penetrated with a 50% by volume solution of 644 and methanol were wetted easily and completely within a few minutes.

Eight test bars were processed as described earlier using the binder-methanol solution. Three test bars failed after the polymer burnout stage of the post-processing, essentially turning to dust when moved. This weakness at the polymer burnout phase was attributed to the polymer coating which apparently leaves too few exposed ceramic surfaces to which the cement can bind. Extreme care was taken to not damage the

127

remaining test bars during post-processing. Also, the initial binder penetration step was altered to try to increase the uptake of cement. Further penetrant was drawn though the bar by placing it on dry towel and dripping more solution onto the surface. The dry towel would draw moisture from the bar thus pulling more material from the surface. This was done on all edges of the bar until no further moisture could be drawn from the bar by dry paper.

The results of mass changes of these test bars were all very consistent. A typical sample gained approximately 0.22 g/g of green material after the drying period. This amount dropped to 0.21 g/g of green material after firing at 200°C, indicating the low moisture content of the dried sample. Following polymer burnout the mass loss was 0.11 g/g of green material, corresponding to a polymer content of 9.6 wt. %. This is in agreement with the expected value of 10 wt. %. When infiltrated a second time a bar typically gained an additional 0.15 g/g of material after drying and firing at 200°C. This results in a typical mass gain of 41% or 0.29 g/g of polymer free material. Initial and final axial measurements are summarized in Table 6.

Table 6. Summary of test bar dimensions

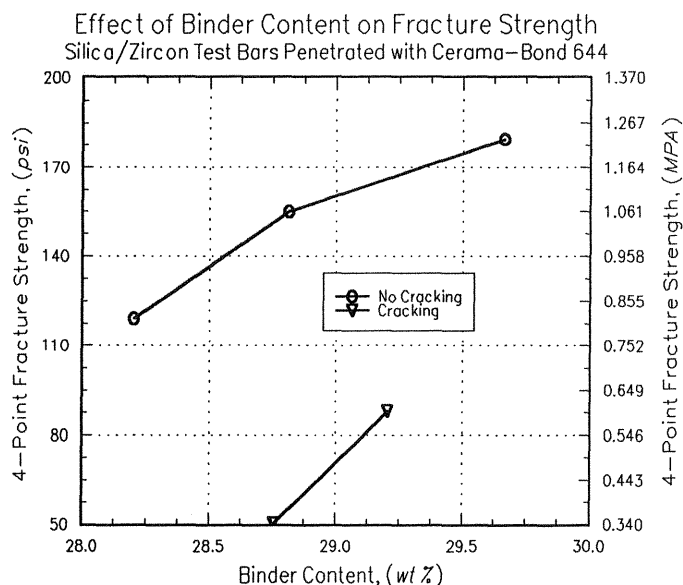| Part #	x, (%)	y, (%)	z, (%)	mass, (%)	Final Density, (%)
14	-2.34	-2.33	-1.32	39.3	45.7
15	-2.40	-2.27	-1.29	41.6	47.2
16	-2.37	-2.46	-1.30	42.2	46.4
20	-4.27	-4.35	-2.00	40.4	47.6
21	-3.41	-3.36	-1.66	41.2	46.5

Figure 2. Effects of binder content.

Figure 2 shows the results of fracture strengths on the parts listed in Table 6. These data clearly show an increase in the resultant strength with increased cement content. The difference between the two sets of data shown in Figure 2 are attributed to the drying

128

conditions for the test bars. Those bars showing a higher fracture strength were dried on an open counter top while the remaining bars were dried in a vent hood with the vent operating. While all parts showed some warpage after drying, only those dried in the vent hood exhibited pronounced cracking of the exposed surfaces. It is presumed these cracks resulted from non-uniform shrinkage of the exposed surfaces due to an increased drying rate caused by the induced air flow of the vent. According to Mujumdar [5], in the drying of clay materials fast drying rates result in a case-hardening. Exposed surfaces shrink about the incompressible core and, as the inner material shrinks, the case will be unable to conform resulting in cracks at weak points. Cracking in these parts occurred primarily along layer boundaries. These large cracks apparently significantly reduced the strength of the bars.

In this series of experiments, both part failure following polymer binder removal and surface cracking during the drying phase severely affected the resultant part properties. In an attempt to eliminate these features of the post-processing modifications were made to the powder material and to the drying step. The powder material was altered, as described previously, by the addition of uncoated ceramic powder to the coated powder stock. This introduced exposed particle surfaces for interaction with the penetrating ceramic cement. The drying step was altered by drying infiltrated parts in a humidity controlled environment. With this modification the effective drying rate could be changed with the intent to try to reduce or eliminate cracking.

Several square pieces made from the two additional powder samples were infiltrated with a *Ludox*® TM 50% by volume solution of 0.3% wt. Dupanol-ME surfactant in water. These cubes were dried in an 80% relative humidity environment at a temperature of 72°F for two days. No cracking was observed in these pieces. Following polymer binder removal all parts were significantly more rigid than samples previously observed.

Test bars, 1"x3"x¼", made from the alumina powder, were infiltrated with the Ludox TM colloid and fully processed as in previous experiments. A portion of the bars were tested for strength. The remaining portion of bars were fired at high-temperature prior to strength testing. A typical bar had a fracture strength of 1.86 MPa (270 psi) before firing and had a fracture strength of 14.55 MPa (2110 psi) after firing for 17 hours at 1000°C. X-ray analysis of the fracture surface fired bars indicated the composition of silica to be homogenous throughout the sample. From mass changes the silica contents of these bars were determined to be about 22% wt. Dimensional shrinkages were approximately 1.0% in all directions. The increase in silica and the small amount of shrinkage resulted in a typical relative density of 61.1%.

A number of turbine core samples were made from the alumina powder and post-processed in the manner just described. A representative core is shown if Figure 3. This part is approximately two inches square and, as can be seen in the figure, the definition of the part is excellent.

Conclusions

The use of ceramic cements has been shown to be an effective path to the production of full strength ceramic pieces from green objects produced by Selective Laser Sintering. While the results are very encouraging there are some issues which must be resolved. Some of these issues which are currently under investigation are the effects of drying conditions, firing cycles, the improvement of penetration, and the type of ceramic cement best suited to the process.
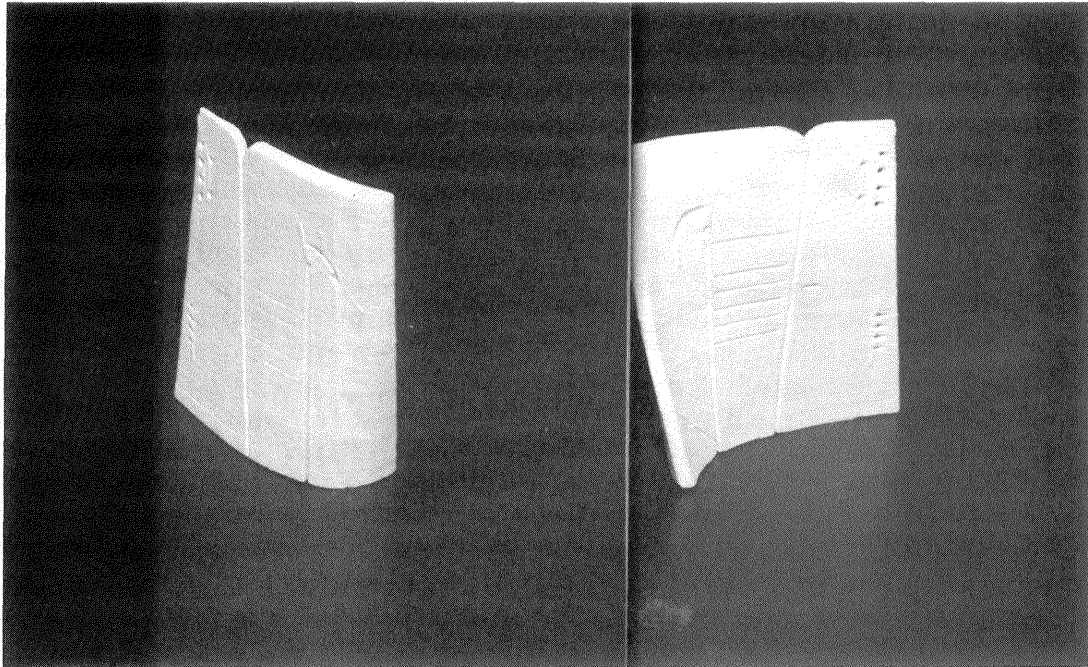
Figure 3. Turbine blade core.

References

1. D.L. Bourell, et.al., "Solid Freeform Fabrication: An Advanced Approach", *Solid Freeform Fabrication Symposium Proceedings*, 1, 1-7 (1990).
2. U. Lakshminarayan, "Selective Laser Sintering of Ceramic Materials", Ph.D. Dissertation, The University of Texas at Austin, 1992.
3. W. Weiss and D.L. Bourell, "Selective Laser Sintering to Produce Ni-Sn Intermetalics", *Solid Freeform Fabrication Symposium Proceedings*, 2, 251-258 (1991).
4. N.K. Vail and J.W. Barlow, "Effect of Polymer Coatings as Intermediate Binders on Sintering of Ceramic Particles", *Solid Freeform Fabrication Symposium Proceedings*, 2, 195-205 (1991).
5. A.S. Mujumdar, Ed., 1987, Handbook of Industrial Drying, (New York: Marcel Dekkar).